Diamond Films and Technology
Vol. 1, No. 3 1992
MYU Tokyo

DFT 0011

Dominance of Intrinsic Phonon Scattering in CVD Diamond

J. E. Graebner and J. A. Herb*

AT&T Bell Laboratories, Murray Hill, NJ 07974 USA
*Crystallume, Inc., Menlo Park, CA 94025 USA

(Received 20 November 1991, accepted 23 December 1991)

Key words: thermal conductivity, CVD diamond, phonon scattering intrinsic scattering, umklapp, low temperature

The thermal conductivity of diamond prepared by a chemical vapor deposition (CVD) process is measured in the temperature range 4–400 K by a new steady-state technique which overcomes the problem of radiative loss of heat from the sample. The conductivity is high at room temperature (17 W/cmK, compared with ~22 for single-crystal diamond) and increases on cooling. The data are fit over the entire temperature range with a model which demonstrates that for $200 < T < 400$ K the phonon scattering is dominated by intrinsic (umklapp) scattering rather than by crystalline defects.

1. Introduction

In nonmetallic solids, thermal energy is generally carried by phonons and the thermal conductivity is limited by the phonon mean free path (mfp) between scattering events. For high-purity single crystals, there is little scattering of phonons from lattice defects or impurities, and the mfp is limited only by the sample boundaries (below ~100 K) or by umklapp phonon-phonon scattering (above ~100 K). The latter becomes rapidly more important as the temperature (and density of phonons) increases, resulting in a conductivity which *decreases* on warming. Single crystals of diamond are an example of materials showing such behavior.[1] Diamond is

unusual, though, in having the highest known conductivity above ~100 K. This is due primarily to the stiffness of the lattice which produces a high acoustic velocity as well as an extremely high Debye temperature (~2000 K). For diamond, room temperature is therefore near the low-temperature limit where umklapp scattering is very weak (large mfp, high conductivity).

Previous reports[2,3] of the temperature-dependent thermal conductivity of polycrystalline CVD diamond films show a relatively low conductivity (3–5 times lower than single-crystal diamond at 300 K) with a positive slope vs temperature in the range 10–300 K, indicating that the mfp is dominated by extrinsic scattering entities such as impurities, lattice defects, and grain boundaries.

The present study of polycrystalline CVD diamond reveals a considerably higher conductivity, with a negative slope between 200 and 400 K which indicates that extrinsic scattering is weak enough to allow umklapp scattering to dominate the mfp.

2. Experiment

The sample is prepared in a specially designed 2.45 GHz microwave plasma-enhanced CVD system. Deposition is performed on silicon wafers under conditions typical of conventional microwave CVD. The sample is $0.035 \times 1.5 \times 1.5$ cm^3 and is optically transparent. The Raman spectrum exhibits a strong peak at 1332 cm^{-1} characteristic of diamond with no apparent features characteristic of graphitic bonding. The full width at half maximum of the peak is 4 cm^{-1}.

The conductivity is measured with a new steady-state technique which allows one to detect and correct for any heat that is exchanged between the sample and its surroundings by thermal radiation. Radiative loss is by far the most common source of error in thermal conductivity measurements at room temperature and above. The new technique is a simple modification of the standard steady-state heated-bar technique in which a bar of material is thermally grounded at one end and heated at the other with power P. The conductivity κ is determined by measuring the temperature gradient $\mathrm{d}T/\mathrm{d}x$:

$$\kappa = P/(A \cdot \mathrm{d}T/\mathrm{d}x), \tag{1}$$

where A is the cross-sectional area of the sample, assumed constant in the region of the ΔT measurement.

Implicit in the definition (Eq. 1) is the assumption that all of the power is conducted through the sample. If, however, the surfaces of the sample (with total area $2L(w + t)$) lose energy at a rate P_{rad}, an effective conductance k_{rad} between the sample and its surroundings at temperature T_0 can be defined as

$$k_{\mathrm{rad}} \approx \frac{P_{\mathrm{rad}}}{(\Delta T)_{\mathrm{av}}} \approx \frac{2\sigma\varepsilon(w + t)L(T_{\mathrm{av}}^4 - T_0^4)}{(\Delta T)_{\mathrm{av}}}, \tag{2}$$

where σ is the Stefan-Boltzmann constant, ε is the emissivity ($0 < \varepsilon \leq 1$), and the average temperature is $T_{av} \approx T_0 + (\Delta T)_{av}$. Expanding T_{av}^4 in a power series, we find $k_{rad} \approx 8\sigma\varepsilon L(w + t)T_0^3$. This effective conductance is to be compared with $k_{cond} = \kappa wt/L$ through the sample, so that the ratio of the two channels for heat flow is

$$R = k_{rad}/k_{cond} = \frac{8\varepsilon\sigma}{\kappa}\left[\frac{W + t}{Wt}\right]L^2T_0^3. \tag{3}$$

Radiation loss clearly is most severe for long, thin plate-like samples with low conductivity at high temperatures. Even for a good conductor such as diamond, radiation can be important. For example, for $\varepsilon = 1$, $w = 1$ cm, $t = 300\ \mu$m, $L = 2$ cm, $\kappa = 10$ W/cmK, and $T_0 = 300$ K, Eq. (3) yields $R = 0.17$; that is, a 17% error is made if radiation loss is not taken into account. The error can easily be far worse if the geometry and/or conductivity are less favorable. Since it is difficult to calculate R accurately because of uncertainties in ε, we use an experimental arrangement which allows us to detect any significant radiation loss while measuring the conductivity. The new procedure employs a second heater (H2 in Fig. 1(a)) located on the sample but close to thermal ground. With power dissipated only in H2, the temperature profile is flat in the absence of radiation but is described by a catenary if radiation loss takes place from all points on the surface. This is illustrated schematically in Fig. 1(b). The radiation loss with H2 powered can be modeled[4] to correct for radiation loss when H1 is powered. For the sample measured here, however, the droop in temperature with H2 powered is at worst (at 400 K) only ~10% of the temperature rise along the sample with H1 powered. With this small correction, the droop may simply be added to the measured slope with H1 powered. At room temperature and below, radiative loss is negligible in this sample, as shown by the flatness of the temperature profile with H2 powered (Fig. 2). Without the use of H2, though, even the order of magnitude of the radiation loss is difficult to determine.

The heaters are deposited directly onto the sample by evaporation (~500 Å of Au on ~2000 Å of Cr, $r \approx 200\ \Omega$). Silver-filled epoxy is used to attach the heater leads (0.0025 cm diam. gold) as well as the thermocouple junctions (Chromel-Constantan, 0.0025 cm diam.). A line of 3–4 thermocouples, Fig. 1(a), may be used for accurate determination of the thermal gradient; a differential thermocouple is more suitable for high-conductance samples where the thermal rise along the sample with H1 powered is much smaller than that at the sample-to-ground joint. For the present sample, depending on the temperature range, the latter can be 10°C for only a 1°C rise along the sample. With the sample in vacuum, and with good temperature control of the thermal ground, a resolution of 0.001°C can be obtained in the vicinity of room temperature. The temperature resolution decreases by a factor of ~10 on cooling to liquid helium temperatures, due to the decrease in the thermopower.

The greatest uncertainty arises in the measurement of the sample thickness because of sample roughness. We estimate an overall uncertainty in the conductivity of ~5%.

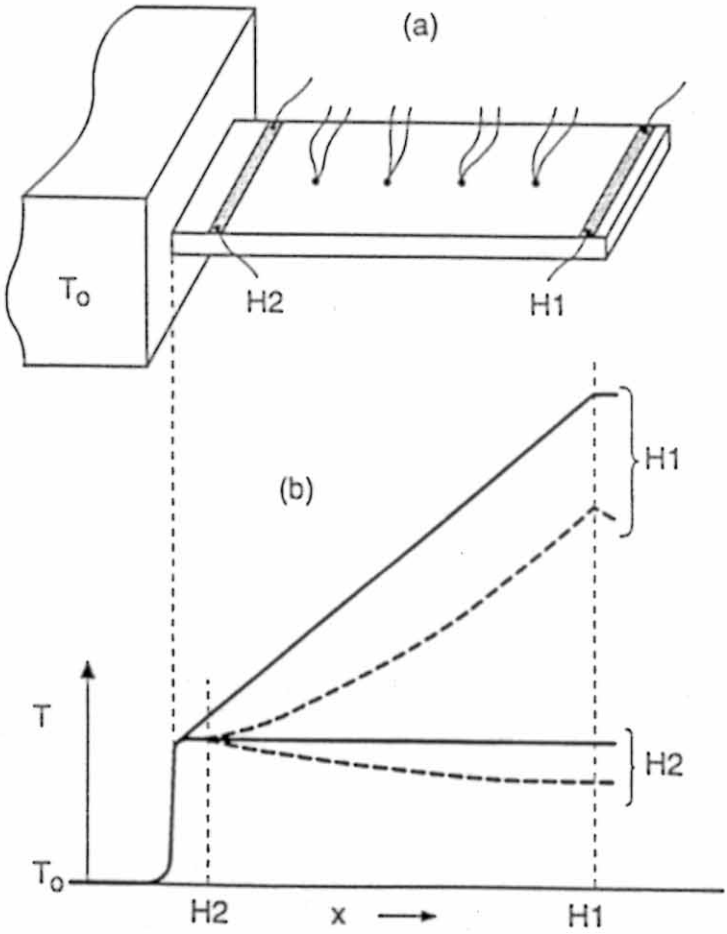

Fig. 1. a) Schematic diagram of a sample mounted for the two-heater heated-bar technique of measuring the thermal conductivity and detecting the presence of radiation loss. The sample is equipped with two thin-film heaters, H1 and H2, and a number of thermocouples. b) Temperature distribution along sample expected for a given power applied to either H1 or H2, for two cases: zero radiation loss from surface of sample (solid straight lines) and severe radiation loss (dashed curves).

3. Results and Analysis

The data are shown in Fig. 3. The conductivity at 300 K is 17 ± 1 W/cmK and the slope is clearly negative for $200 < T < 400$ K, with $d(\ln \kappa)/d(\ln T) = -0.73$. At the highest temperature (~400 K), the conductivity of the film approaches that of high-quality (type IIa) bulk single crystals,[5-7] also shown in Fig. 3 and in greater detail in Fig. 4. Below 200 K, the conductivity drops off rapidly with a broad dip centered at ~30 K, while a comparable dip is observed in the single-crystal data at ~10 K.

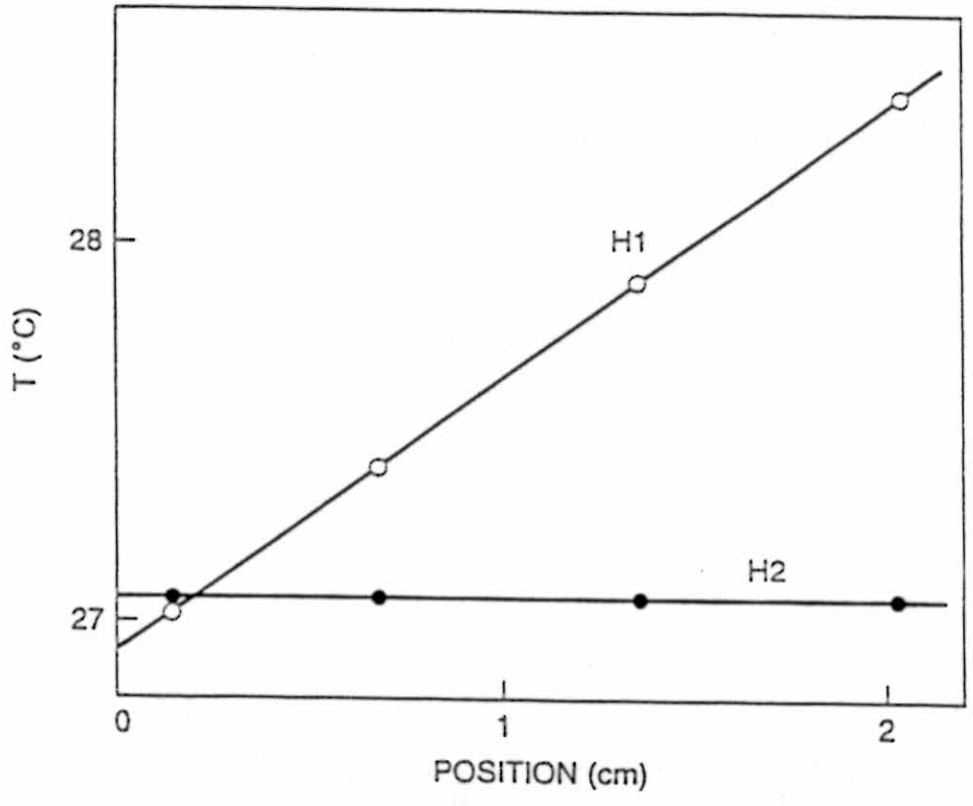

Fig. 2. Thermocouple data at room temperature with power dissipated in H1 and (slightly more) in H2. The flatness of the temperature profile for H2 powered shows that radiation loss is negligible for this sample at this temperature. The slope determined with power in H1 is used with the power, thickness, and width to obtain the thermal conductivity according to Eq. 1.

To understand the magnitude and temperature dependence, one may model the conductivity within the Debye phonon approximation[1] with various contributions to the phonon scattering which are adjusted to fit the data. The conductivity can be expressed as an integral over temperature T and phonon frequency ω:

$$\kappa = \frac{k_B}{2\pi^2 v}\left[\frac{k_B}{\hbar}\right]^3 T^3 \int_0^{\theta/T} \frac{\tau(x) x^4 e^x \, dx}{(e^x - 1)^2}, \tag{4}$$

where v is an appropriately averaged velocity of sound,[8] k_B and $\hbar$ are Boltzmann's and Planck's constants, respectively, θ is the Debye temperature,[9] $x = \hbar\omega / k_B T$, and $\tau^{-1}(x)$ is the scattering rate at temperature T for a phonon of frequency ω. If one makes the usual assumption that scattering rates are independent,[1] the rates τ_i^{-1} are additive. We have used the following contributions to τ^{-1}:

1. At the highest temperature, phonon-phonon umklapp scattering must be taken

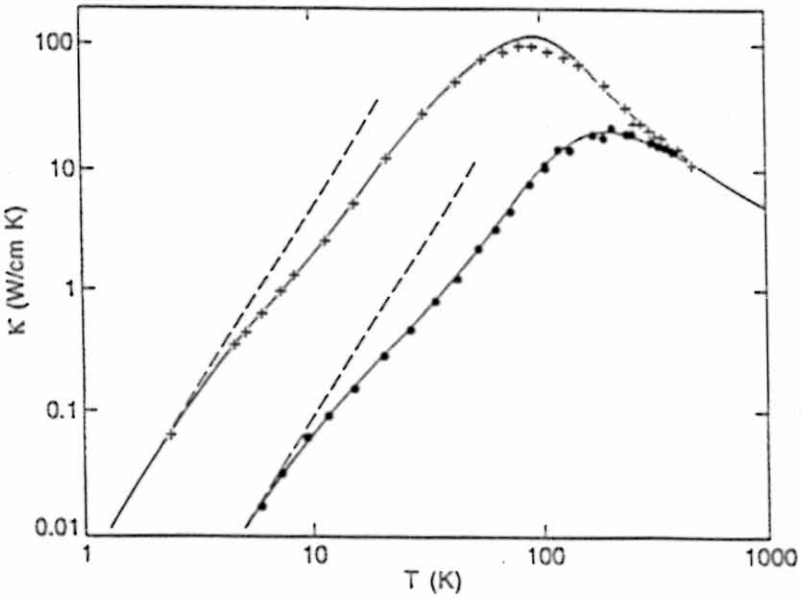

Fig. 3. Thermal conductivity of CVD diamond (circles) and single-crystal type-IIa natural diamond (crosses, Ref. 5). The solid lines are the fits calculated from Eqs. 4–9 with the parameters listed in Table 1. The dashed lines indicate T^3 dependence.

into account. High-temperature measurements in the highest purity single crystals available are usually used as an approximation of the ideal conductivity. We have used data on type II_a crystals, including very recent work[7] above 500 K, and we find better agreement with the form $\tau_u^{-1} \sim \omega^2 T \exp(-1/T)$ than with previously used expressions,[1,2,10] such as $\omega^2 T^2 \exp(-1/T)$ or $\omega^2 T^3 \exp(-1/T)$. Specifically, we use

$$\tau_u^{-1} = A_u x^2 T^3 \exp(-B_u/T). \tag{5}$$

2. Point-defect scattering from isolated atoms of different mass, either isotopes or different elements, gives rise to a Rayleigh ω^4 term:

$$\tau_R^{-1} = A_R x^4 T^4. \tag{6}$$

3. For an extended defect such as the strain field around a vacancy, one also expects Rayleigh scattering for wavelengths that are large compared to the defect. At high frequencies, interference effects become important and eventually the cross section becomes independent of frequency, i.e., the geometrical limit. For a spherical object of diameter D, the Rayleigh scattering varies as ω^4 and the crossover occurs at $\omega_c = v/D$. We use a simplified version[11] of the theoretical models for such scattering:

$$\begin{aligned} \tau_{Rco}^{-1} &= A_{Rco} x^4 T^4 && \omega < \omega_c \\ &= A_{Rco} \omega_c (\hbar / k_B)^4 && \omega > \omega_c \end{aligned} \tag{7}$$

4. Boundary scattering is important at the lowest temperatures where other scattering mechanisms are generally weak. Assuming diffuse scattering at the surface of the sample or at the internal surfaces between grains, one typically uses[12,13]

$$\tau_b^{-1} = v/\alpha d, \tag{8}$$

where d is the sample or grain size. The factor $\alpha = 1.12$ for a square sample/grain.
5. At the highest frequency and temperatures, some of the above scattering mechanisms lead to unphysically small mean free paths. To avoid this, we calculate the sum of those scattering rates $\Sigma\tau_i^{-1}$ and then require an upper limit by calculating

$$\tau(x) = r/v + (\Sigma\tau_i^{-1})^{-1}, \tag{9}$$

where r is a minimum mean free path, typically an interatomic dimension.[14]

Many other scattering mechanisms have been used for different materials.[14,15] Our approach here is to use the smallest number of terms necessary to fit the data at hand. Our primary goal is to test the importance of umklapp scattering in this CVD diamond, i.e., whether all other scattering is weak enough that intrinsic scattering is observable.

The single-crystal data in Fig. 4 is used first to optimize the umklapp term.

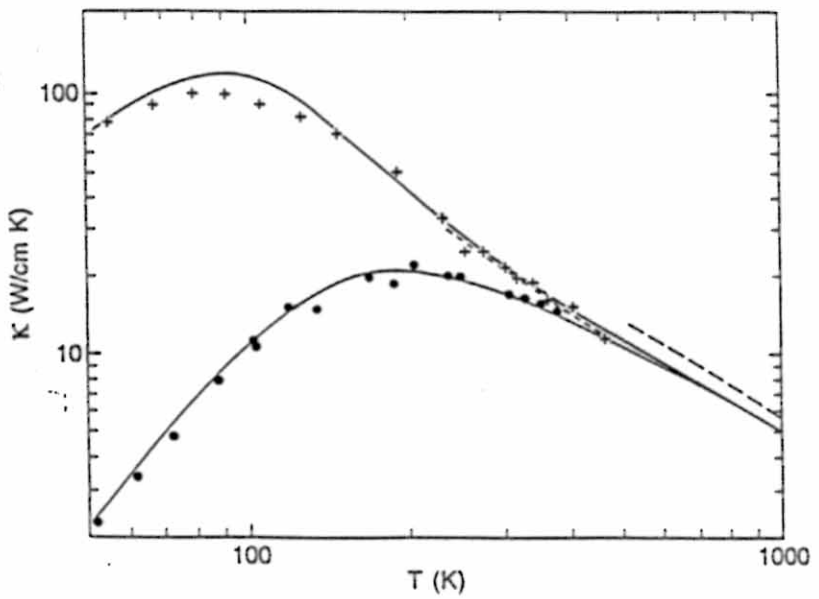

Fig. 4. Expanded view of the high-temperature portion of Fig. 3. Also shown are data on type-IIa diamond from Ref. 6 (short-dashed line) and Ref. 7 (long-dashed line).

Because of the good agreement between the data of Refs. 5 and 6 in the region of overlap (200–450 K), we have concentrated the umklapp fit on the temperature interval 150–450 K. The higher-temperature data ($T > 500$ K) lie parallel to the calculation, which suggests that the latter data come from a somewhat more perfect sample. We leave unanswered the question of the ultimate conductivity of a defect-free diamond sample. Our primary concern here is the temperature dependence, which can be reproduced very well by Eq. 5, a form which has also been used successfully for alkali halides.[16,17]

The parameters used in the fits are listed in Table 1. The parameters are fairly independent of each other because of the tendency for each one to be important in only a limited range of temperature. The umklapp parameters A_u and B_u are different from those used previously, not only because of the different temperature dependence in Eq. 5 but also because we are fitting to data over a much wider temperature range. A_u and B_u are determined from the single-crystal data and then used without change for the CVD diamond data. The Rayleigh scattering is large enough to account for isotope scattering (a mass defect formula[18] for natural-abundance ^{13}C predicts $A_R = 0.0044\ s^{-1}\ K^{-4}$, compared to our two values of 0.025 and 0.015), plus some other source of point defects. The cut-off Rayleigh scattering due to extended defects is considerably stronger but approximately what one would expect for scattering by the strain field around vacancies. Either the 10 Å or 30 Å diameter D of the defect is a reasonable size for the strain field around a vacancy. An alternate scattering mechanism that fits the data equally well in the region of the dip is resonance scattering by localized phonons around a defect. In this resonant scattering picture, the dominant phonons near the dip (10 K in single crystals, 30 K in CVD) have energies of ~ 4 kT = 4–10 meV. These are typical of the energies of localized phonon modes associated with vacancies.[17] Demonstrating conclusively which model is more appropriate would require more exhaustive sampling of specimens with different concentrations of known defects, which is beyond the scope of the present work. The minimum mean free path $r = 3$ Å makes little difference in the

Table 1

Parameters used in the fit to data in Figs. 3 and 4. The parameters are defined in Eqs. 4–9. A double period indicates no change.

	Single Crystal	CVD
Θ (K)	2030	—
v (cm/s)	1.32×10^6	—
A_u ($s^{-1}\ K^{-3}$)	640	—
B_u (K)	470	—
A_R ($s^{-1}\ K^{-4}$)	0.025	0.015
A_{Rso} ($s^{-1}\ K^{-4}$	10	15
D (cm)	3×10^{-7}	1×10^{-7}
d (cm)	0.2	0.0035
r (cm)	3×10^{-8}	—

calculated conductivity below 500 K, and at 1000 K results in an increase of only ~10%.

The largest difference between the two samples lies, of course, in the frequency-independent scattering rate. The values of 2 mm and 35 μm, respectively, correspond quite well to the size of the bulk single crystal and the average grain size of the polycrystal. The latter is difficult to estimate because it varies as a function of distance from the starting surface, but examination of the top surface shows a grain size of ~50 μm.

The main conclusion is that the data for both materials are fit well with a small set of reasonable parameters and that in both cases the scattering from defects or boundaries is small enough to reveal the intrinsic umklapp scattering with its unique negative slope.

4. Conclusions

High-quality CVD diamond has been found to have a thermal conductivity at room temperature that is only 25% less than single-crystal type-IIa diamond. Measurements over two orders of magnitude in temperature allow us to model the conductivity in detail. While some of the scattering mechanisms are not unambiguously determined without more exhaustive work, it is clear that, in the temperature range 200–400 K, the scattering of phonons by defects is small enough that intrinsic (umklapp) scattering dominates the conductivity.

References

1) R. Berman: *Thermal Conduction in Solids*, (Oxford University Press, Oxford, 1976).
2) D. T. Morelli, C. P. Beetz and T. A. Perry: J. Appl. Phys., 64 (1988) 3063.
3) T. R. Anthony, J. L. Fleischer, J. R. Olson and D. G. Cahill: J. Appl. Phys., 69 (1991) 8122.
4) H. S. Carslaw and J. C. Jeager: *Conduction of Heat in Solids*, Second Ed. (Clarendon Press, Oxford, 1959) p. 139.
5) R. Berman and M. Martinez: Diamond Research 1976, Suppl. to Ind. Diam. Rev., p. 7.
6) E. A. Burgemeister: Physica, 93B (1978) 165.
7) J. W. Vandersande, C. B. Vining and A. Zoltan: "Long" Direction Data, *Electrochemical Soc. Proc. 91-8 Sec. Int. Symp. on Diamond Materials*, (1991) 443.
8) J. W. Vandersande: Phys. Rev., B13 (1976) 4560.
9) D. L. Burk and S. A. Friedburg: Phys. Rev., 111 (1958) 1275.
10) V. I. Nepsha, N. F. Reshetnikov, Yu. A. Klyuev, G. B. Bokii and Yu. A. Pavlov: Sov. Phys. Dokl., 30 (1985) 547.
11) J. W. Schwartz and C. T. Walker: Phys. Rev., 155 (1967) 969.
12) H. B. Casimir: Physica, 5 (1938) 495.
13) P. Carruthers: Rev. Mod. Phys., 33 (1961) 92.
14) G. Slack: *Solid State Physics*, ed. F. Seitz and D. Turnbull (Academic Press, New York, 1979) Vol. 34, p. 1.
15) P. G. Klemens: *Solid State Physics*, ed. F. Seitz and D. Turnbull (Academic Press, New York, 1958) Vol. 7, p. 59.

16) C. T. Walker: Phys. Rev., 132 (1963) 1963.
17) J. W. Schwartz and C. T. Walker: Phys. Rev., 155 (1967) 959.
18) R. Berman: *Thermal Conduction in Solids*, (Oxford University Press, Oxford, 1976) p. 74.